

AD-A081 853

SACLANT ASW RESEARCH CENTRE LA SPEZIA (ITALY)
ENVIRONMENTAL ACOUSTICAL MODELLING AT SUPREME ALLIED COMMANDER.--ETC(U)
NOV 79 F B JENSEN; W A KUPERMAN
SACLANTCEN-SR-34

F/6 20/1

UNCLASSIFIED

NL

ADP-1
ADP-2



END
DATE
FILMED
4 80
DTIC

14

SACLANTCEN REPORT SR-34

NORTH ATLANTIC TREATY ORGANIZATION
SACLANT ASW Research Centre
Viale San Bartolomeo 400, I-19026 San Bartolomeo (SP), Italy.

tel: national 0187 503540
international + 39 187 503540
telex: 271148 SACENT I

Supreme Allied Commander, Atlantic,
Anti-Submarine Warfare Research Center

6 ENVIRONMENTAL ACOUSTICAL MODELLING AT (SACLANTCEN)

10 by
Finn B. Jensen and William A. Kuperman

11
1 November 1979

12441

This report has been prepared as part of Project 19.

Accession For	
NTIS G...I	<input checked="" type="checkbox"/>
ODC TAB	<input type="checkbox"/>
Unannounced	<input type="checkbox"/>
Justification	
BY	
Distribution/	
Availability Codes	

APPROVED FOR DISTRIBUTION

B.W. Ythall

B.W. YTHALL
Director

A

312.950

[Handwritten mark]

TABLE OF CONTENTS

	<u>Pages</u>
ABSTRACT	1
INTRODUCTION	3
1 PROPAGATION MODELLING AT SACLANTCEN	5
1.1 Overview of the models	5
1.2 Descriptions of the models	6
1.3 Inter-model comparison	8
2 MODELS AND EXPERIMENTAL DATA	15
2.1 Model/data comparison	15
2.2 Conclusions from model/data studies	19
3 SPECIAL MODEL APPLICATIONS	23
3.1 Propagation over a sloping bottom	23
3.2 Seismic propagation	28
4 NOISE MODELLING AT SACLANTCEN	33
CONCLUSION	39
REFERENCES	40

List of Figures

1. Contoured reflection loss versus grazing angle and frequency for a layered bottom (Model Result)	10
2. Inter-model comparison for shallow water environment	11
3. Inter-model comparison for deep water environment	12
4. Environment handled by the SNAP model	15
5. Model predictions and experimental data for shallow water area in northern Mediterranean	16
6. Environmental input to SNAP for modelling shallow water area in southern Mediterranean	18
7. Predicted and measured depth-averaged loss versus frequency for environment presented in Fig. 6	18
8. Environmental input to SNAP for modelling coastal water area in eastern Atlantic	20
9. Measured and predicted transmission-loss contours for environment presented in Fig. 8	20
10. Predicted loss versus range for down-slope propagation	24
11. Predicted loss versus range for up-slope propagation	25
12. Sound propagation in a wedge-shaped ocean	26
13. Environmental input to FFP for modelling seismic versus waterborne propagation paths	29

TABLE OF CONTENTS (Cont'd)List of Figures (Cont'd)

	<u>Pages</u>
14. Predicted loss versus range for seismic and waterborne paths	30
15. Predicted loss versus frequency for seismic and waterborne paths	30
16. Deep and shallow-water model environments for calculating surface-generated noise levels	34
17. Environmental input to shallow-water noise model	35
18. Predicted noise and field intensities versus depth	35
19. Modal depth function for first 6 modes	36
20. Spatial correlation function of noise for two different receiver depths	36

ENVIRONMENTAL ACOUSTICAL MODELLING AT SACLANTCEN

by

Finn B. Jensen and William A. Kuperman

ABSTRACT

↓
The SACLANT ASW Research Centre's programme in environmental acoustic modelling is presented, with emphasis on applications to coastal water environments. A brief description of the acoustic models in use at the Centre is given together with an inter-model study that demonstrates the consistency among the models. A sequence of examples from data/model comparisons indicates that the models can indeed describe shallow-water propagation. These studies have also demonstrated the collective role of models and data to describe coastal-water regions acoustically. Finally some results from simulation studies of propagation over a sloping bottom, seismic propagation, and the spatial distribution of surface-generated noise are presented.
↑

INTRODUCTION

During recent years, SACLANTCEN has been conducting an extensive experimental and theoretical research programme in underwater environmental acoustics. The present report is concerned with the Centre's theoretical modelling effort in this area and summarizes its modelling capabilities by presenting a sequence of results from recent investigations. No equations are presented but there are adequate references so that the interested reader can obtain the pertinent mathematics.

The Centre's environmental acoustic modelling effort has been primarily concerned with coastal or shallow water areas. By either of these terms we mean, roughly, a propagation environment where sound repeatedly interacts with the ocean bottom. Hence, we are not only interested in continental shelf areas but also in propagation over a continental slope and even in the coupling of sound from deep to shallow water or the reverse.

The driving factor in the modelling programme at the Centre has been the excellent computer facilities available to the modelling group. This group consists of a few scientists and programmers and is a major user of a time-shared Univac-1106 system. Some modelling is also being done on Hewlett Packard HPMX-21 computers. The most important feature of all models discussed in this report is that they are all running in both interactive and batch modes on the Univac-1106 system and they are easily accessible and usable to not only the modelling group but also to anyone else at the Centre.

The report is divided into four main sections. Chapter 1 describes the models in use at the Centre and the philosophy used in acquiring, modifying and using these models. We also present some comparisons between models. In Chapter 2 we present examples of a comparison between models and broadband experimental data for three different shallow-water areas. The results indicate that we have, at present, a good (but not complete) understanding of the physics of sound propagation in coastal waters. Having gained some confidence in the applicability of the models from this data/model comparison we can then use the models as tools to study different propagation phenomena. In Chapter 3 we present examples from two different investigations: propagation over a sloping bottom and seismic propagation in coastal water areas. Finally, Chapter 4 deals with the spatial distribution of surface-generated noise in shallow water.

PROCESSED PAGE BLANK-NOT FILMED

1 PROPAGATION MODELLING AT SACLANTCEN

1.1 Overview of the models

An overview of the propagation models in use at SACLANTCEN is given in Table 1. Seven models are listed, of which the first three are wave models

TABLE 1 PROPAGATION MODELS IN USE AT SACLANTCEN

MODEL NAME	MODEL TYPE	APPLICATIONS							
		SHALLOW WATER				DEEP WATER			
		LF		HF		LF		HF	
		RI	RD	RI	RD	RI	RD	RI	RD
SNAP	mode	hatched	hatched	hatched	hatched	hatched	hatched	hatched	hatched
FFP	fast field	hatched	hatched	hatched	hatched	hatched	hatched	hatched	hatched
PAREQ	parabolic eq.	hatched	hatched	hatched	hatched	hatched	hatched	hatched	hatched
GRASS	ray			hatched	hatched	hatched	hatched	hatched	hatched
FACT	ray			hatched	hatched	hatched	hatched	hatched	hatched
NISSM II	ray			hatched	hatched	hatched	hatched	hatched	hatched
RAIBAC	ray			hatched	hatched	hatched	hatched	hatched	hatched
		(1)	(2)	(3)	(4)	(5)	(6)	(7)	(8)

LF: low frequency (< 500 Hz)

HF: high frequency (> 500 Hz)

RI: range-independent environment

RD: range-dependent environment

and the rest are ray models. This distinction is important, since only wave models are without theoretical frequency restrictions in their applicability, and hence are models that handle both diffraction and reflection processes in a correct frequency-dependent fashion. Ray theory is essentially a high-frequency approximation to the wave equation. The difference between the three wave models (SNAP, FFP, PAREQ) lies mainly in the solution techniques applied. In all cases the starting point is the wave

PROCESSED PAGE BLANK-NOT FILMED

equation, which, by assuming the environment to be range-independent, can be solved either in terms of normal modes (SNAP) or by a direct numerical integration with the use of an FFT algorithm (FFP). Finally, by assuming propagation to take place within small angles (about $\pm 20^\circ$) with respect to the horizontal, the "elliptic" wave equation can be transformed into a "parabolic" equation amenable to a numerical marching-solution technique (PAREQ). Emphasis in this report will be on the wave models, which are most applicable when studying the interaction of sound with the ocean bottom. Later on in this chapter we shall briefly discuss the origin of all models and give appropriate references.

To indicate with some precision the type of ocean environment for which a given model should be used, we have classified environments according to water depth, frequency, and environmental complexity, as shown in Table 1. Here shallow water indicates all water depths for which sound interacts significantly with the ocean bottom. The separation frequency of 500 Hz between the low- and high-frequency regimes is arbitrarily chosen.

When indicating the applicability of a model to a given type of environment, we take into consideration limitations in the underlying theory. Thus ray models are applicable only to high-frequency propagation, and only some models (SNAP, PAREQ, GRASS) can handle a range-dependent environment. When indicating a model's practicality we consider exclusively the running time. Thus the time increases with both frequency and water depth for some models (SNAP, PAREQ), while the time is relatively independent of these parameters for the other models. Likewise, running time is proportional to the number of profiles in a range-dependent environment for SNAP and GRASS, while PAREQ takes essentially the same time for range-dependent and range-independent environments.

Full box shading in Table 1 means that a model is applicable as well as practical. On the other hand, if a box is only partially shaded, it means that the model is applicable with caution (theoretical limitations), or that running times are excessive. The above judgements are, of course, relative. That is, this suite of models was originally chosen such that every column had at least one partially-filled box; then for columns that did not originally have a fully-shaded box, we selected the model we felt was the most practical and denoted it by a fully-shaded box. For a column where more than one box is fully shaded, we actually use the model that is most convenient, taking into consideration running time, input/output options, and the simplicity of using the model.

1.2 Descriptions of the models

Below we briefly describe the models, giving references and an occasional comment when necessary to minimize the ambiguity of Table 1.

SNAP [1] is a normal-mode model based on a computer program originally developed at the US Naval Research Laboratory [2,3]. The original program has been completely restructured and modified to create a propagation model particularly suited for modelling needs at SACLANTCEN. Thus SNAP has been designed to handle a shallow-water ocean environment as realistically as possible, including slight range dependence ("adiabatic approximation") in environmental parameters. The model is highly automated with a flexible input/output structure. If a column of Table 1 has more than one fully-shaded box with SNAP included, SNAP is the preferred program in our model studies because: i) it is the easiest to use; ii) it has the greatest number of output options; iii) its modularized architecture allows it to be easily modified for new uses when necessary.

FFP [4,5] is a complete numerical solution of the wave equation and hence also includes the near field. The model residing at the Centre originates from Columbia University [5]; this particular model includes propagation of both compressional and shear waves and is therefore suitable for seismic studies. In the FFP model the shear velocity may take on any physical value, whereas in SNAP the shear velocity should be less than about 500 m/s (typical of most coastal water sediments).

PAREQ [6,7] is a parabolic equation model; the computer program running at the Centre is a modified version of the one developed by the Acoustic Environmental Support Detachment of the US Navy [8]. The Centre's model (PAREQ) not only handles a variable profile in depth and range but also allows the bottom depth and bottom structure to vary in range. The bottom is characterized by compressional speed, density, and attenuation, of which the speed may vary arbitrarily with depth. PAREQ is not only resident on the Centre's Univac-1106 but has also been installed on a Hewlett Packard HPMX-21 computer.

GRASS [9] is a range-dependent ray trace program originally developed at the US Naval Research Laboratory.

FACT [10] was developed at the Acoustic Environmental Support Detachment of the US Navy and has been modified to accept bottom-loss versus grazing-angle. Additional plot options have also been added.

NISSM II [11] was developed at the US Naval Underwater Systems Center and not only calculates propagation loss but also other quantities such as reverberation, probability of detection, etc. Additional plot options have been added to the original version.

RAIBAC [12] was developed at SACLANTCEN; it is a fast ray-trace model that calculates spatially-averaged propagation loss with the averaging performed by incoherent summation of the contributions of individual ray bundles to each of the rectangular cells into which the depth/range plane is divided. This model also contains a reverberation package.

Table 2 summarizes the main input/output features of the models; that is, the table indicates both the type of environment a given model can handle (through the input) and the type of calculation that can be performed (through the output). Thus Table 2 provides the necessary additional information on the models for choosing between them when two or more models in Table 1 are shown to be applicable to the same ocean environment. Note that there are no two models with the same input/output features.

The input table shows that three models can handle a range-dependent environment. We also see that bottom properties can be entered either as an angle-dependent reflection loss or by directly entering physical properties such as speed, density, and attenuation for the various layers. In the latter case a distinction is made between fluid bottoms, fluid bottoms with a solid basement, and the general case of multilayered solid bottoms. Furthermore, one model (FFP) is particularly suited for modelling propagation in the Arctic since it can handle the presence of a surface ice layer.

Table 2 also shows that while many models can handle sea-surface roughness, only one model (SNAP) includes bottom roughness. Finally, source/receiver beam pattern can be entered in three of the models.

Before commenting on the output options, we should mention that the Centre possesses a bottom-loss model [13,14] that handles a solid, multilayered, damping bottom. This model is being used to provide reflection-loss versus grazing-angle and frequency, to be used as input for ray models. An example is given in Fig. 1. First is shown the environmental input to the bottom-loss model (Fig. 1a) and, below, the computed loss in dB contoured versus grazing-angle and frequency. The shaded regions indicate losses higher than 5 dB. We see that the bottom layering results in a high variation of reflection losses with frequency and angle for frequencies above 200 Hz. At lower frequencies (longer wavelengths) the sediment layer of Fig. 1a becomes transparent to an incoming wave, and the bottom then acts as if homogeneous.

Returning to Table 2, we see that all models can output loss versus range. Furthermore, most models can give contoured loss versus depth and range, and also give sound-speed profile plots. However, it is clear from Table 2 that the SNAP model provides the greatest number of output options.

1.3 Inter-model comparison

Returning to Table 1, we note that models designated applicable to a particular environment should give the same answer. First let us look at the shallow-water example displayed in Fig. 2, where a simple isovelocity shallow-water environment is considered. The water depth is 100 m and the source and receiver are at mid-depth. The bottom is characterized by a sound speed of 1550 m/s, a density of 1.2 g/cm^3 , and an attenuation of

TABLE 2 SUMMARY OF INPUT/OUTPUT FEATURES

INPUT	SNAP	FFP	PAREQ	GRASS	FACT	NISSW II	RAIBAC
RANGE-DEP. ENVIRONMENT							
BOTTOM LOSS VS ANGLE							
LAYERED FLUID BOTTOM							
LAYERED FLUID BOTTOM WITH SOLID BASEMENT							
LAYERED SOLID BOTTOM							
SURFACE ICE LAYER							
SURFACE ROUGHNESS							
BOTTOM ROUGHNESS							
SOURCE/RECEIVER BEAM PATTERNS							
OUTPUT							
LOSS VS RANGE							
LOSS VS DEPTH							
DEPTH-AVERAGED LOSS VS RANGE							
DEPTH-AVERAGED LOSS VS FREQUENCY							
CONTOURED LOSS VS DEPTH AND RANGE							
CONTOURED LOSS VS FREQUENCY AND RANGE							
CONTOURED DEPTH-AVR. LOSS VS FREQ. RANGE							
MODAL GROUP VELOCITY VS FREQUENCY							
MODAL PHASE VELOCITY VS FREQUENCY							
MODE FUNCTIONS VS DEPTH							
PHASE OF FIELD VS DEPTH							
INTENSITY OF FIELD VS ARRIVAL ANGLE							
SOUND SPEED VS DEPTH							
CONTOURED SPEED VS DEPTH AND RANGE							
RAY TRACE							
PULSE PROPAGATION VS TIME AND RANGE							

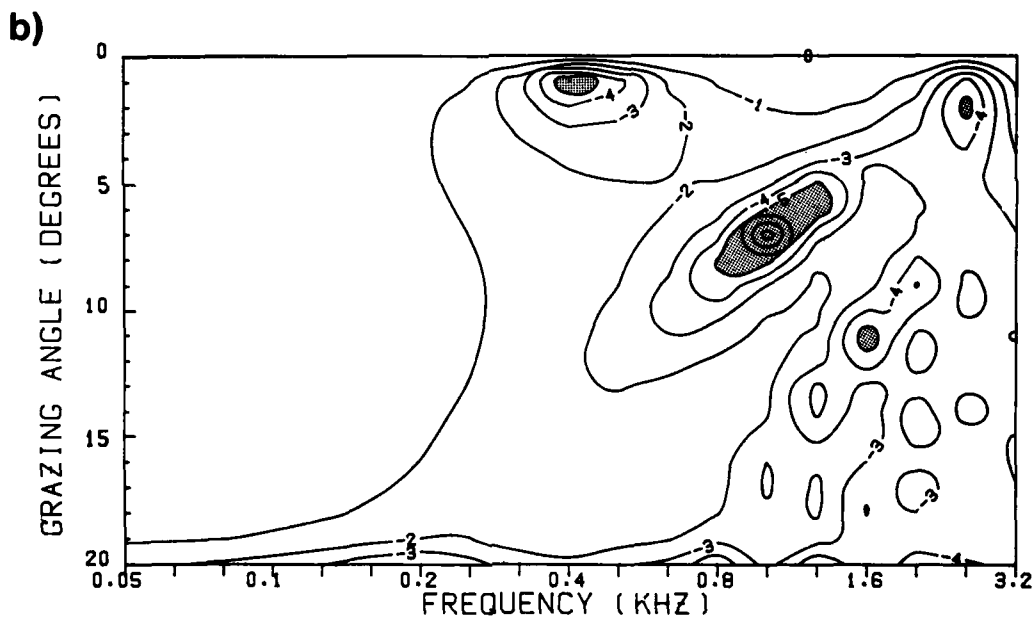
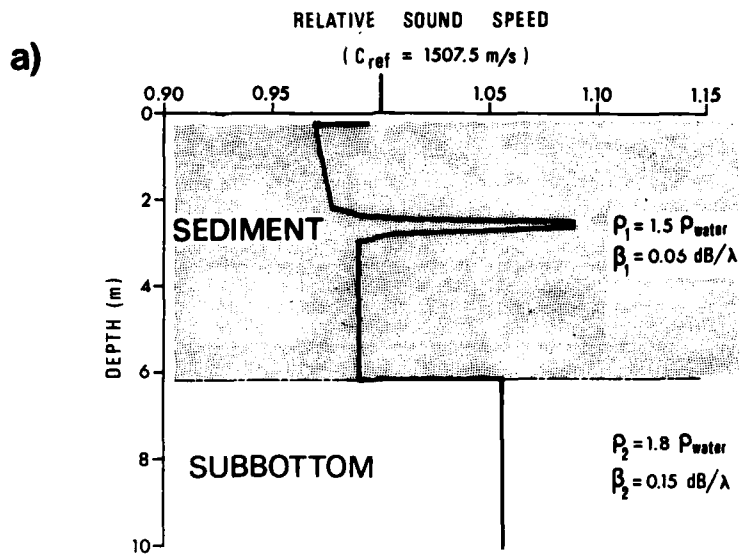


FIG. 1 CONTOURED REFLECTION LOSS VERSUS GRAZING ANGLE AND FREQUENCY FOR A LAYERED BOTTOM (Model Result)

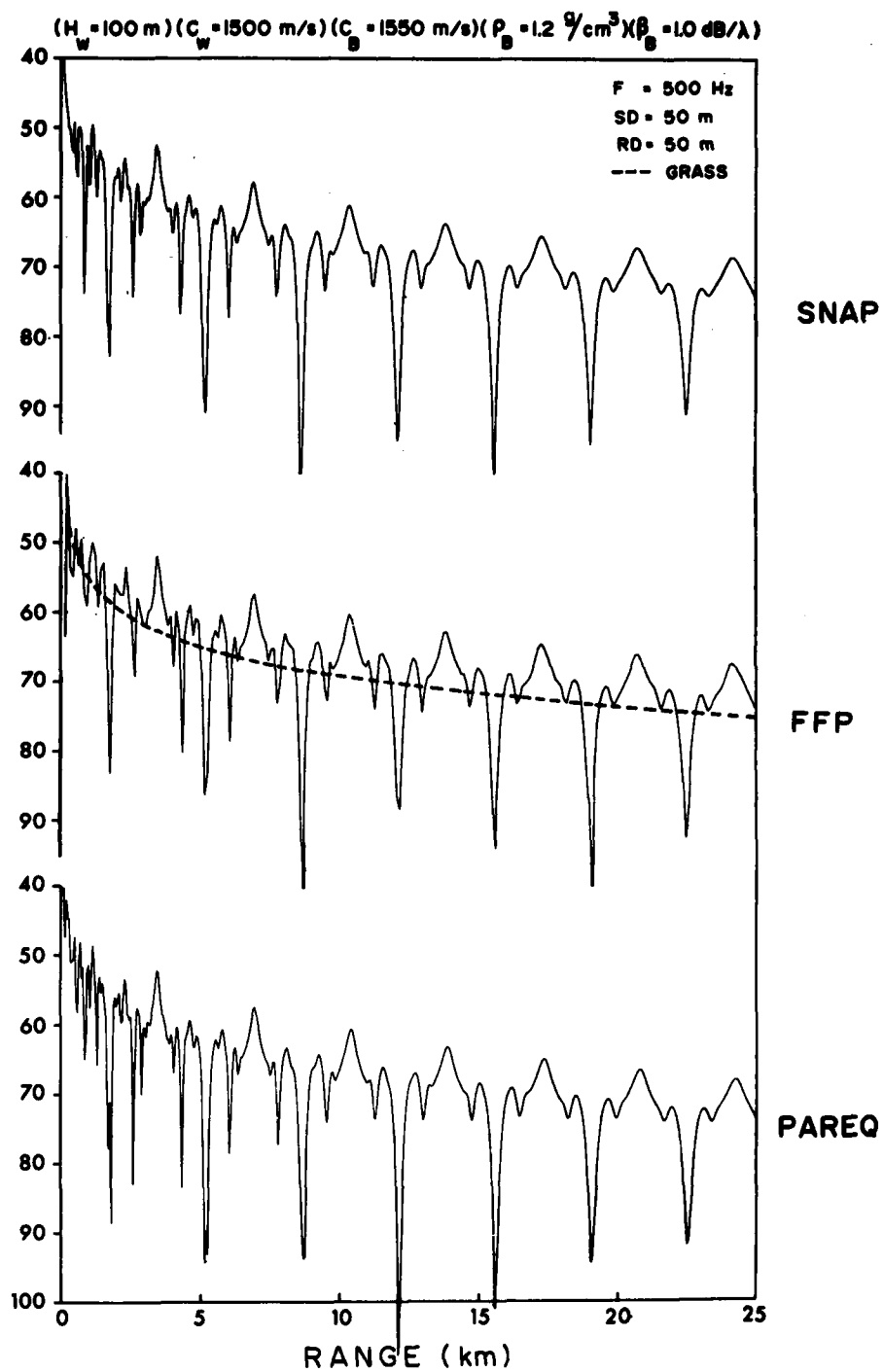


FIG. 2 INTER-MODEL COMPARISON FOR SHALLOW WATER ENVIRONMENT

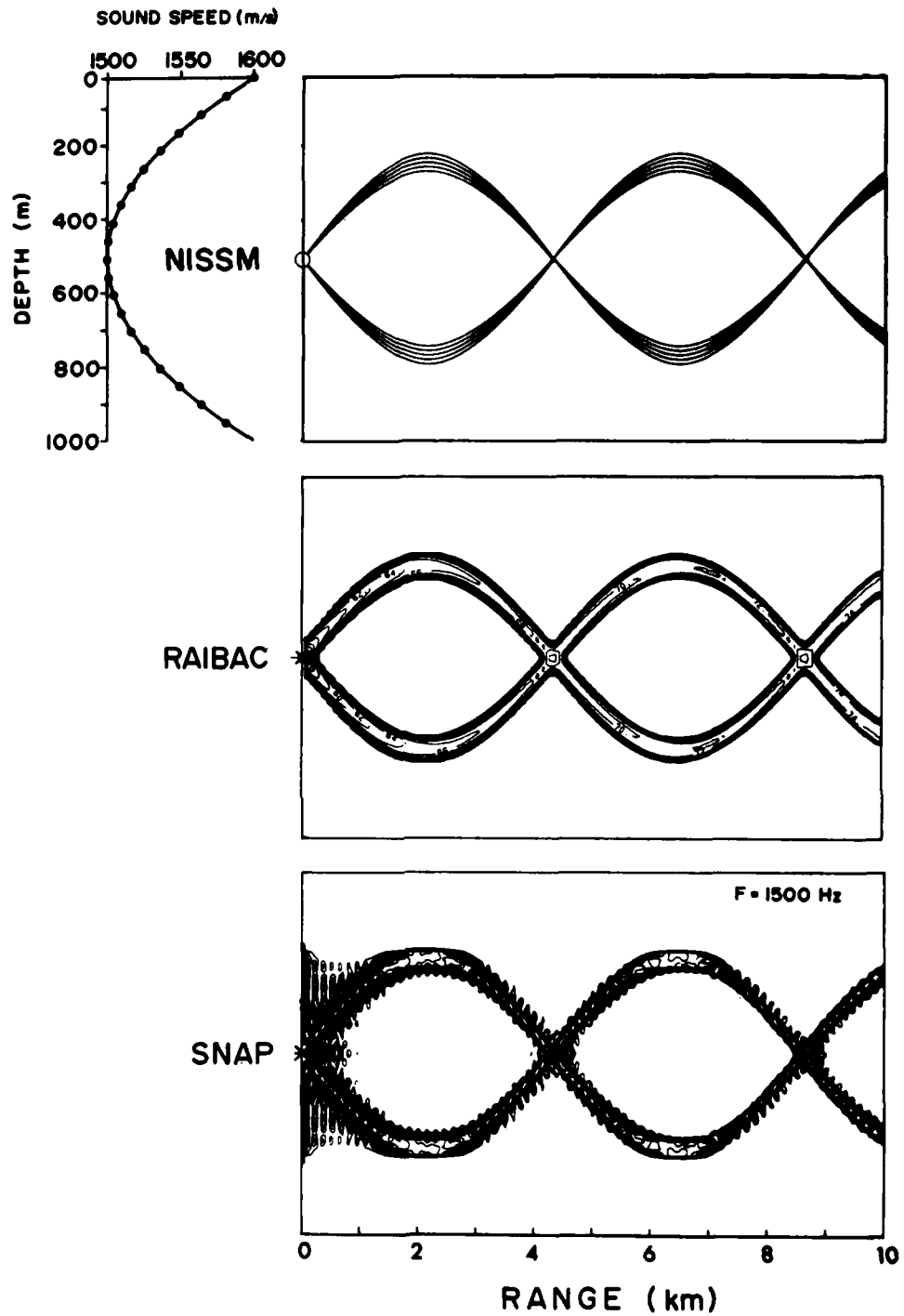


FIG. 3 INTER-MODEL COMPARISON FOR DEEP WATER ENVIRONMENT

1 dB/wavelength. The three wave models are compared and one observes that the outputs are virtually identical. This corresponds to comparing all models in application column (1) of Table 1. Since this example is for 500 Hz, which is our arbitrary boundary between high frequency and low frequency, the ray models indicated in application column (3) should also work. Plotted with the FFP results is the statistical output from GRASS. One does not expect a ray program to give the same detailed interference pattern in shallow water but the output of GRASS indicates approximately the same mean level as that of the wave models. Actually GRASS gave the closest result to the wave models but the other ray models were also reasonably close.

Figure 3 depicts a deep-water application. We have chosen an idealized sound-speed profile, as shown, and we study the SOFAR type propagation as displayed by the NISSM ray trace output for up- and down-going 2° beams centred around $\pm 10^\circ$ from the horizontal. RAIBAC and SNAP have also been exercised for this situation, but for those two models we have contoured loss versus depth and range. These are not ray-trace plots but they look like them. In the case of RAIBAC (a ray-trace program) the levels fall abruptly when the field point are outside the ray paths indicated by NISSM. In the SNAP output, we see that we can obtain a ray-like picture from a wave-theoretic model. The interval (70 to 90 dB) of loss levels was chosen so that extremely-high loss contours (low field strength) do not clutter up the display. The difference between the SNAP results and the ray-program outputs at close ranges is a wave-diffraction effect. By selecting modes that correspond (in the ray-mode analogy) to up- and down-going 2° beams we are thereby abruptly cutting off the other modes; in a sense this corresponds to a situation where a point source is behind a baffle containing two diffraction slits. We also note that for the wave theory result (SNAP) the field in reality is non-zero outside the ray paths and falls off as a function of frequency; hence there is some field strength in the so-called "shadow" region.

Finally, in regard to the models discussed in this chapter, it is important to point out that they are all resident on the same computer installation and easily operable in an interactive mode.

2 MODELS AND EXPERIMENTAL DATA

The comparison of model outputs with experimental data has the two-fold purpose of validating a given model and of giving increased understanding of the environmental factors governing sound propagation in a given area. In recent years SACLANTCEN has collected broadband propagation data in various coastal-water regions, and these data have all been, or are currently being, modelled by applying one or more of the models described earlier.

2.1 Model/data comparison

In this section we show representative examples of broadband propagation data averaged in 1/3 octave bands for three different shallow-water areas. In all cases the data are compared with outputs from the SNAP model, though other models were also used to assured model consistency. Before proceeding to the model/data comparison, we illustrate the actual physical environment handled by SNAP.

As shown in Fig. 4, the environment is a half space sub-divided into three layers: a water column of depth H_0 , a sediment layer of thickness H_1 , and a semi-infinite sub-bottom. In the water column the sound speed $c_0(z)$ is allowed to vary arbitrarily with depth, while density ρ_0 and volume attenuation β_0 are taken to be constant over depth. The sediment layer is treated in exactly the same way: an arbitrary sound-speed profile $c_1(z)$, a constant density ρ_1 , and a constant volume attenuation β_1 . The sub-bottom, on the other hand, is treated as a solid with depth-independent properties: c_{2S} is the shear speed and β_{2S} the shear attenuation; c_2 is the compressional speed, ρ_2 the density, and β_2 the compressional attenuation.

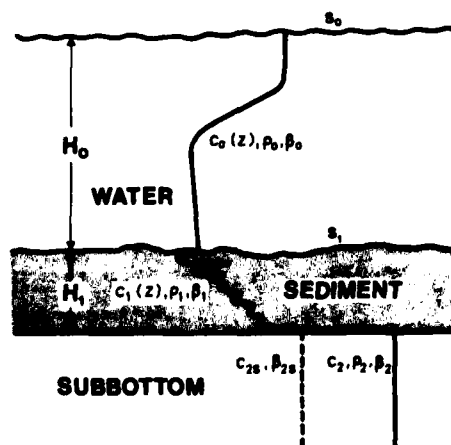


FIG. 4 ENVIRONMENT HANDLED BY THE SNAP MODEL

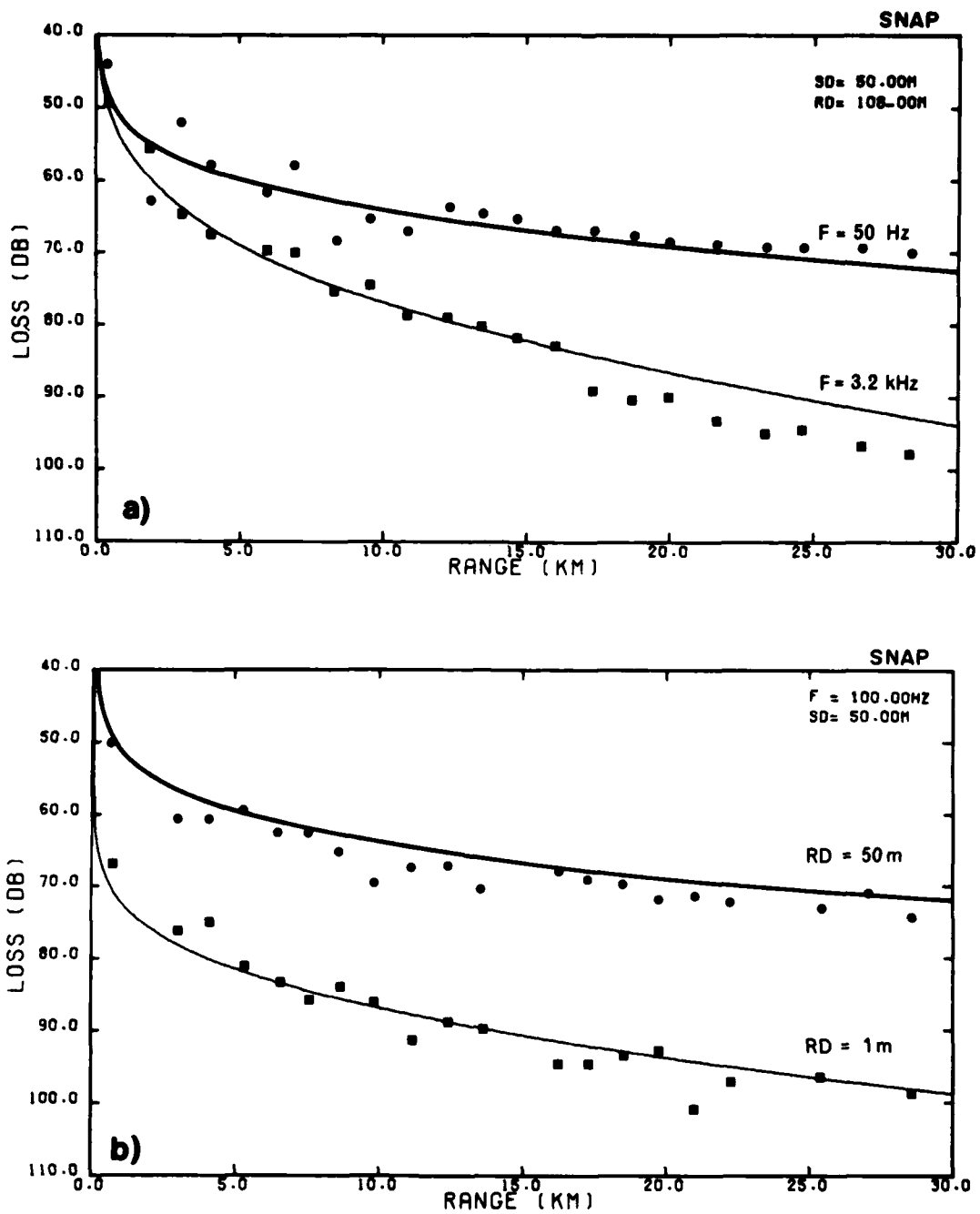


FIG. 5 MODEL PREDICTIONS (Full lines) AND EXPERIMENTAL DATA (Dots) FOR SHALLOW WATER AREA IN NORTHERN MEDITERRANEAN (RD = Receiver Depth, SD = Source Depth, F = Frequency)

Furthermore, both sea surface (pressure release) and sea floor are treated as rough boundaries, with the rms roughness heights given by the parameters s_0 and s_1 , respectively. In case of a range-dependent environment, the full range is divided into a certain number of segments, each with different range-independent properties.

When demonstrating the capability of an acoustic model by comparison with experimental data it is important to use data with a good depth and range coverage, examples of which will be shown below. The first example shows data collected in the northern Mediterranean in 110 m of almost isothermal water. The bottom structure, which is well-known from numerous cores taken during sea trials, is that illustrated in Fig. 1. Note the existence of a 6 m thick layer (clay) with a sound speed less than that for water, and with a thin high-speed layer (sand) embedded in it. By using this bottom as input to the SNAP model, we obtain the agreement shown in Fig. 5 between model predictions (full lines) and experimental data (dots).

As we see from Fig. 5a, the agreement is good for the two widely-different frequencies (50 Hz and 3.2 kHz), an agreement that could not have been obtained using an over-simplified homogeneous bottom as input to the model. Figure 5b shows results for two different receiver depths: 1 and 50 m. The source depth is 50 m and the frequency 100 Hz. Again the agreement between theory and experiment is excellent, and we see that the field intensity close to the surface is 20 to 30 dB below the intensity in the middle of the water column at all ranges. Thus we see from this particular example that sound propagation in a complicated ocean environment can be accurately modelled when all environmental parameters are adequately known. However, it does not always work out like that.

The next example shows data from a different area of the Mediterranean. Here we have propagation data for two seasons, as indicated by the sound-speed profiles in Fig. 6. The bottom in this area is quite homogeneous and it was therefore modelled as a semi-infinite solid bottom with the properties given in the figure 6. Here only the compressional speed C_c and the density were determined from core measurements, while the other parameters were guessed on the basis of information retrieved from the literature and the fact that the model output should agree with measured data.

The comparison between theory and experiment is shown in Fig. 7 for the two different profiles of Fig. 6. We have here plotted the depth-averaged loss versus frequency at a fixed range of 30 km. As we see, the agreement is reasonable for the summer profile, while the model predicts too low a loss at all frequencies for the winter profile. This is a slightly disturbing result, taking into consideration the many "free" parameters involved, e.g. shear speed, attenuation, and boundary roughness. However, by choosing these parameters within realistic limits, it was not possible to improve agreement for the winter profile without also affecting the summer results for the worse. Thus, we have no explanation at the moment for this kind of one-sided disagreement between theory and experiment displayed in the upper graph of Fig. 7.

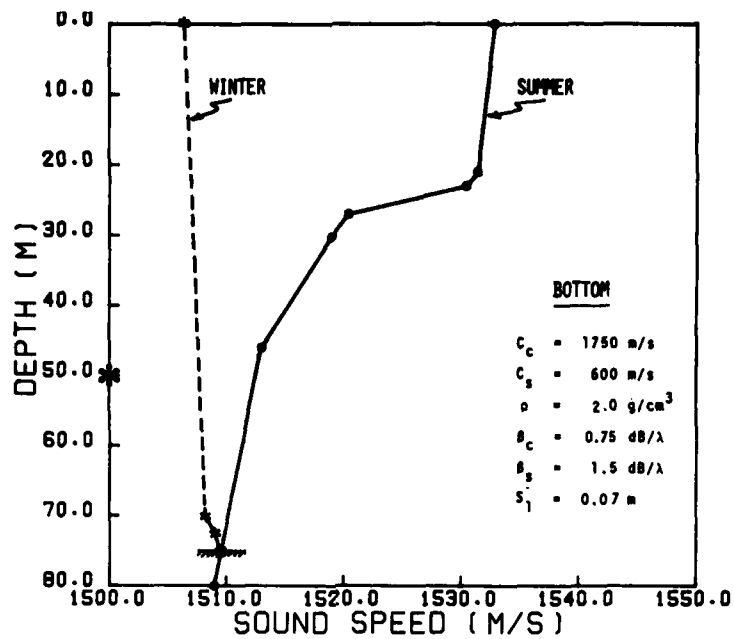


FIG. 6 ENVIRONMENTAL INPUT TO SNAP FOR MODELLING SHALLOW WATER AREA IN SOUTHERN MEDITERRANEAN

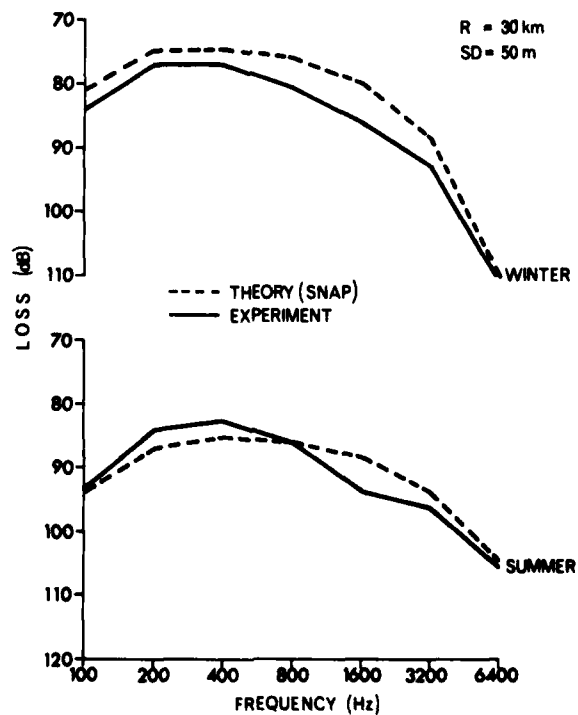


FIG. 7 PREDICTED AND MEASURED DEPTH-AVERAGED LOSS VERSUS FREQUENCY FOR ENVIRONMENT PRESENTED IN FIG. 6

The last example of model/data comparison is related to a coastal water area in the eastern North Atlantic in summer. The profile is shown in Fig. 8, together with the bottom properties (estimated from grab samples) used as input to the SNAP model. It is a homogeneous sand bottom with a substantial bottom rms roughness of 0.4 m (sand dunes).

The experimental data are displayed in Fig. 9a as contoured loss versus range and frequency for a source depth of 50 m and a receiver depth of 59 m. The optimal propagation frequency is seen to be approximately 250 Hz. The model result is shown in Fig. 9b, displayed in exactly the same way. Here we see that the optimal frequency increases slightly with range, being around 300 Hz at 80 km. By comparing the two contour plots we notice an extraordinary agreement between theory and experiment. Thus the maximum deviation is only a few decibels for data covering as much as seven octaves of frequencies and a range of more than 80 km. This result was obtained after including shear waves in the bottom and a pronounced sea floor roughness.

2.2 Conclusions from model/data studies

As a result of the extensive data/model comparison done at the Centre we have reached the conclusion that even though we cannot generally predict absolute levels accurately over a wide frequency range, we can accurately predict such important features as optimal propagation frequency, optimal source/received depth, etc. However, this conclusion is based on the assumption that we have a detailed knowledge about the ocean environment, and, for coastal-water areas, particularly about the ocean bottom. Here we touch on one of the key questions associated with acoustic modelling today, since detailed environmental information is generally not available, and the more sophisticated the models become, the more detailed environmental input is needed.

The problem is therefore how to obtain sufficiently detailed environmental information to be able to predict propagation in a given coastal-water area. Concerning the water column, it is relatively easy to obtain sound-speed profiles well sampled in range and time. Bottom properties, on the other hand, are very difficult to obtain. One approach can be excluded immediately, namely that of local reflectivity measurements. To illustrate this point we return to Fig. 9. Here the estimated bottom parameters lead to a critical angle of about 20° . We know, however, that most of the energy propagates at even shallower angles with respect to the horizontal. Thus around the optimal frequency of 200 Hz the important propagation paths have grazing angles less than 5° , which means that each path interacts with the bottom from 50 to 100 times over a range of 80 km. If we arbitrarily settle for a 3 dB agreement between theory and experiment as being satisfactory, we see that we must know the reflectivity of the bottom at any point along the 80 km track to an accuracy of 0.03 dB. Reflectivity measurements to that kind of accuracy at sea are not possible, particularly not at very small grazing angles. Thus, reflectivity measurements is not the solution in shallow-water environments, where sound repeatedly interacts with the bottom.

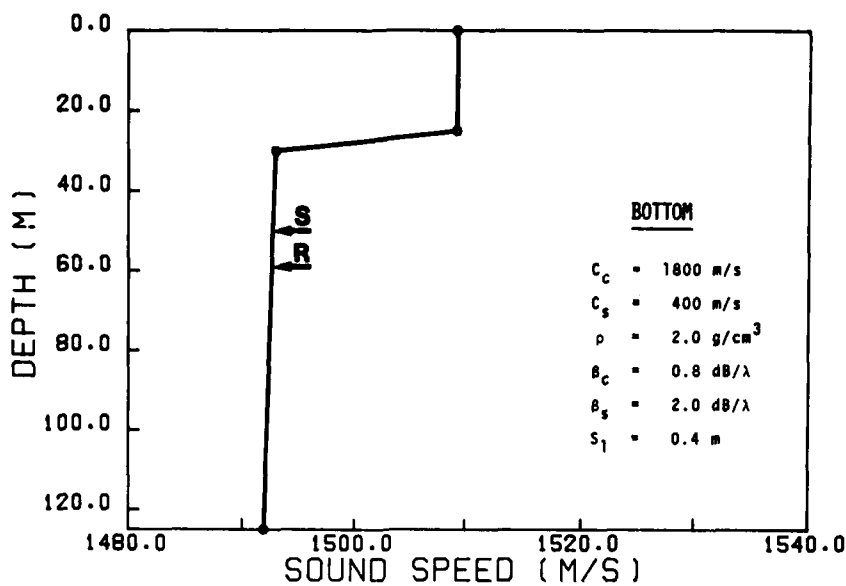


FIG. 8 ENVIRONMENTAL INPUT TO SNAP FOR MODELLING COASTAL WATER AREA IN EASTERN ATLANTIC

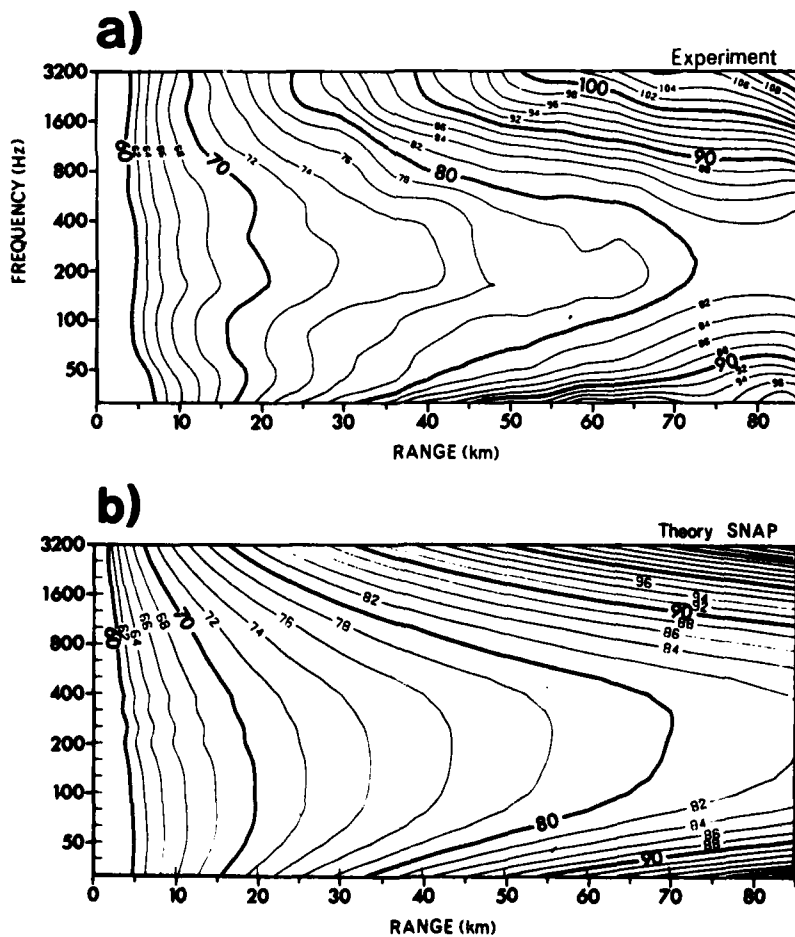


FIG. 9 MEASURED AND PREDICTED TRANSMISSION-LOSS CONTOURS FOR ENVIRONMENT PRESENTED IN FIG. 8

Not even bottom cores can give us the necessary detailed information about the bottom, for two reasons: first, one cannot extract the acoustic properties from a core corresponding to an in-situ reflectivity with a 1% accuracy. Second, cores give information only about the very upper layers of the bottom.

How then do we determine the bottom properties? We feel that the only feasible way is a combination of a) sound-speed profiles and bathymetry, b) cores for determining the upper bottom layering, c) a seismic-profiling experiment for the deeper layering, d) a broadband propagation experiment, and e) a sophisticated propagation model.

Some initial rough information on bottom composition, layering, etc. is needed, and this information can best be obtained from coring and seismic profiling. Then the data/model comparison is used to "fine-tune" bottom parameters until an acceptable agreement is obtained between theory and experiment. For broadband experimental data with a good depth and range coverage, the "solution" for the ocean bottom should be unique. However, with too many unknown parameters and a limited data set, one may find several combinations that seem to describe equally well the measured acoustic properties of the bottom. Therefore the more initial information that is available about the bottom, the better we can determine the actual bottom composition.

Thus we need the acoustic experiment to determine the sea-floor characteristics. Then what do we use acoustic models for in terms of actual propagation predictions? To answer this question we have to distinguish between deep- and shallow-water environments. In deep water, where bottom interaction is of minor importance, we can confidently predict propagation by just knowing the sound-speed structure in the water column. In shallow water we should be able to make predictions for various seasons and sea states, once bottom properties are known. The bottom properties are best determined on the basis of summer data, since the profile is downward refracting, causing maximum sound interaction with the bottom.

The above approach to the use of acoustic models is exactly what has been followed at the Centre, and the result is that today we have a pretty good knowledge about the bottom composition in all areas where SACLANTCEN has been doing experiments.

3 SPECIAL MODEL APPLICATIONS

Our data/model and inter-model studies have provided us with the confidence to use these models as tools to study more complicated propagation phenomena. In this chapter we present some results from two such investigations.

3.1 Propagation over a sloping bottom

The ocean environments considered so far have all been range-independent (horizontally stratified), which in fact is a good approximation to the actual environment in many areas. However, when either water depth, sound-speed profile, or bottom composition varies significantly over the propagation path, the propagation characteristics of a given area cannot in general be modelled satisfactorily without taking into account the range-dependent properties of the environment.

To demonstrate the capabilities of the range-dependent models residing at the Centre (SNAP, PAREQ, and GRASS), we have chosen to study propagation over a sloping bottom at a sufficiently low frequency that phenomena such as mode cut-off and mode conversion can be investigated. Considering the frequency chosen (25 Hz), only SNAP and PAREQ are applicable (see Table 1). Of these two models, PAREQ is a range-dependent model that should include mode-coupling effects. SNAP, on the other hand, is range dependent in the "adiabatic" approximation [1] and does not take into account mode coupling. For that reason SNAP can be expected to work correctly only for slight range dependence, which in this case means gradual bottom slopes. In fact the following examples of up-slope and down-slope propagation serve the purpose of illustrating to what extent the simplified "adiabatic" theory can handle a range-dependent environment.

We first consider down-slope propagation for the environment shown in the upper part of Fig. 10. The propagation path is 40 km, starting with a shallow 10 km path of 50 m depth. Two different slopes are considered, 0.85° and 8.5° , where the latter corresponds to nearly the steepest slope encountered at the edge of the continental shelf. The water is taken to be isovelocity with $C_w = 1500$ m/s, while the bottom is characterized by a speed of 1600 m/s, a density of 1.5 g/cm³, and an attenuation of 0.2 dB/wavelength. The frequency is 25 Hz and both source and receiver are at 25 m depth.

In the shallow part (50 m depth) only a single mode exists, while four modes can be present in the deep part (350 m). Propagating over the slope of 0.85° , as shown on the middle graph of Fig. 10, the two models give almost identical results. Since no interference pattern is present, we can conclude that no more than one mode is excited over the propagation path. Going to the steeper slope of 8.5° (lower graph), the two models again

PRECEDING PAGE BLANK-NOT FILMED

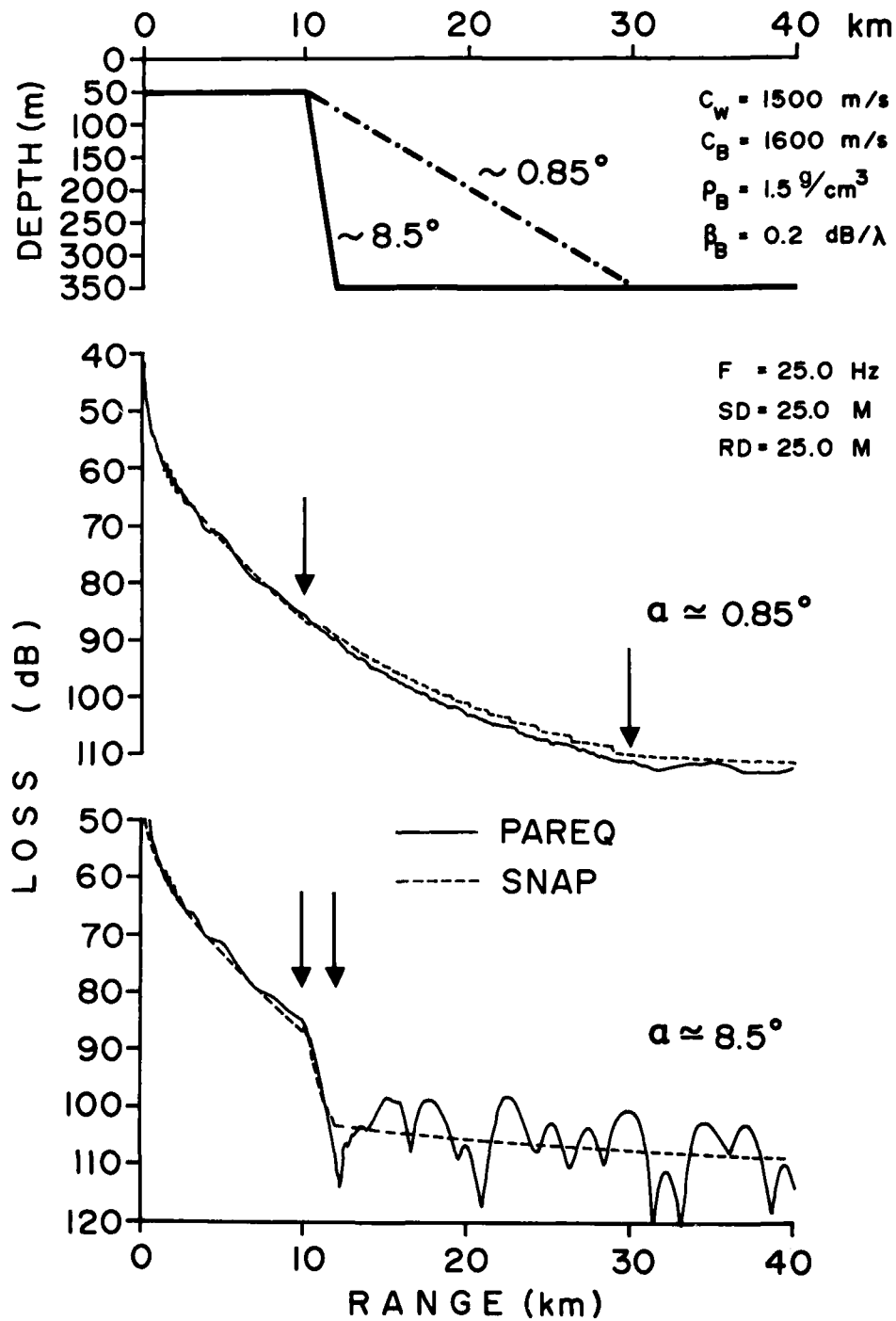


FIG. 10 PREDICTED LOSS VERSUS RANGE FOR DOWN-SLOPE PROPAGATION

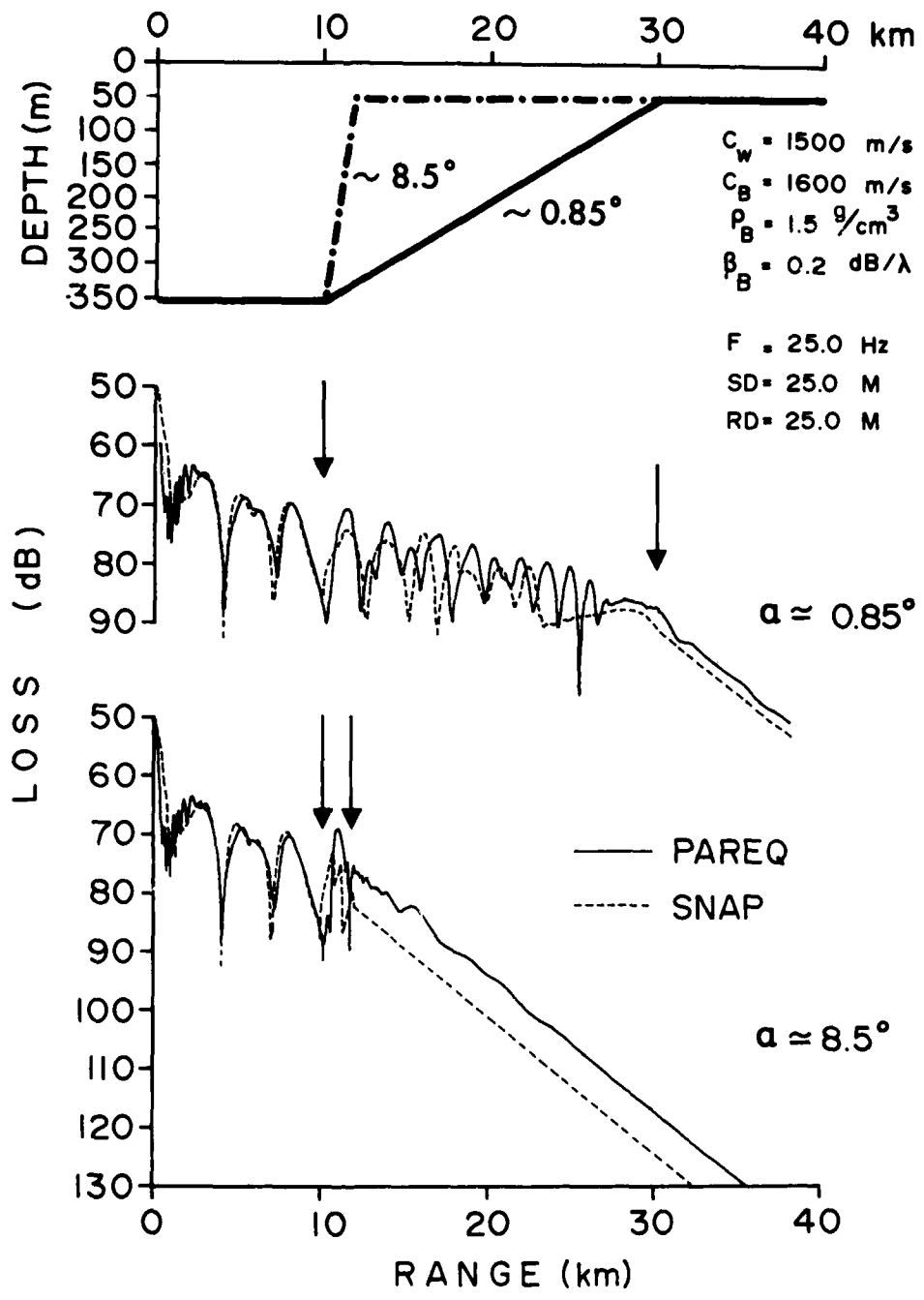


FIG. 11 PREDICTED LOSS VERSUS RANGE FOR UP-SLOPE PROPAGATION

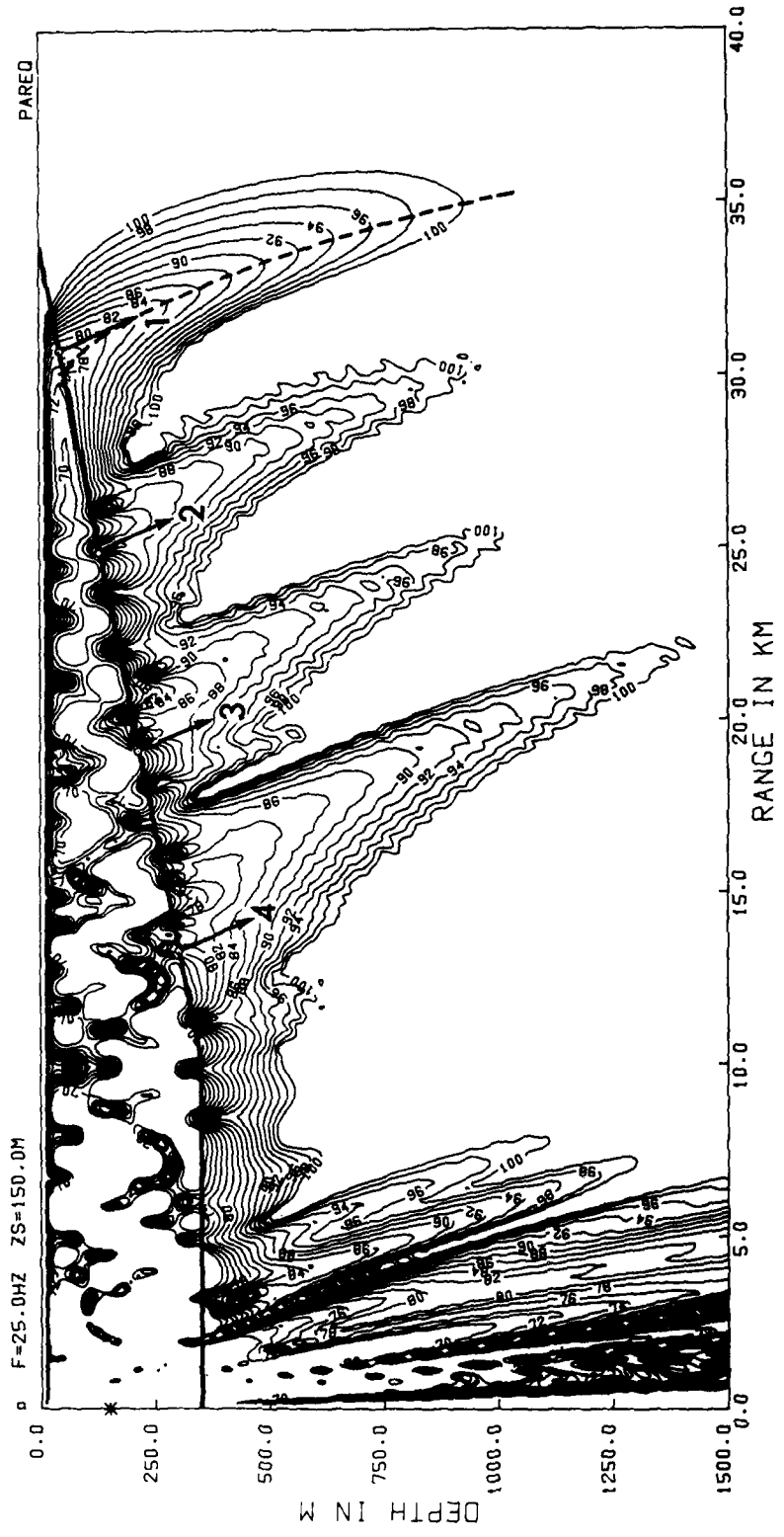
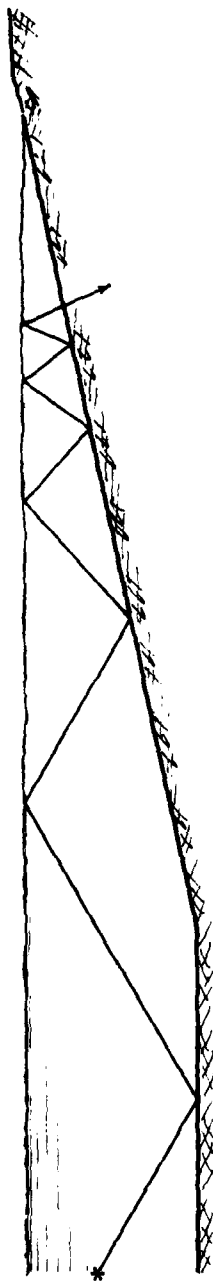


FIG. 12 SOUND PROPAGATION IN A WEDGE-SHAPED OCEAN

agree well on mean levels, but in this case PAREQ shows a pronounced interference pattern beyond the slope. Thus PAREQ indicates that mode coupling takes place, i.e. energy from the one mode excited before and on the slope goes into the excitation of higher modes after the slope. As pointed out earlier, this mode conversion effect is not included in SNAP, but since mean levels agree quite well, we may conclude that the adiabatic range dependence in SNAP works well for down-slope propagation, even for large slopes.

Turning to the case of up-slope propagation for the same environment, see Fig. 11, we start off with the presence of four modes in the deep end of the track and we would here expect to see the three highest-order modes being cut off during propagation up the slope. In the middle graph of Fig. 11 we see the result for a gentle slope of 0.85° . The agreement between the two curves is satisfactory, even though SNAP indicates a cut-off of the second mode a few kilometres too early. Note the high loss in the shallow part of the track beyond 30 km.

The lower graph shows less agreement between the two model predictions. For this slope (8.5°), SNAP predicts too high a loss beyond the slope, indicating that the "adiabatic" theory breaks down for very steep slopes. This was also to be expected, but it is interesting to note that the "adiabatic" approximation handles down-slope propagation better than up-slope propagation.

This particular physical problem of model cut-off during up-slope propagation has been treated recently, both theoretically and experimentally, by Coppens and Sanders [15,16]. They considered propagation in a wedge-shaped ocean, and they were particularly interested in studying how energy propagating in a given mode leaves the wedge, i.e. does energy leak into the bottom continuously with range or does it disappear more abruptly close to the cut-off depth for the mode considered? Both theory and experiment showed that the latter mechanism is the correct one: that energy contained in a given mode leaks down into the bottom as a well-defined beam originating from the place at the bottom that corresponds to the cut-off depth for a particular mode. To verify this phenomenon we have run the wedge problem with PAREQ, using the same water and bottom properties as in Figs. 10 and 11. The result is given in Fig. 12, where we have contoured loss versus depth and range. The frequency is 25 Hz and the source depth is 150 m. The water/bottom interface is indicated by the heavy line starting at 350 m depth and moving towards the surface beyond 10 km. The slope is 0.85° .

Before interpreting the contour plot, let us have a look at the simplified sketch in the upper part of Fig. 12. Using the ray/mode analogy, a given mode can be associated with up- and down-going rays with a specific grazing angle. The sketch indicates a ray corresponding to a given mode. As sound propagates up the slope, the grazing angle for that particular ray (mode) increases, and at a certain point in range the angle exceeds the critical angle at the bottom, meaning that the reflection loss becomes very large and that the ray essentially leaves the water and starts propagating in the bottom. The point in range where this happens corresponds to the cut-off depth for the equivalent mode.

Returning to the loss plot, contouring is done in the range 70 to 100 dB in steps of 2 dB, and the dB interval is chosen so as to bring out clearly the features we are looking for. Thus, high-intensity regions (loss < 70 dB) are given as blank areas within the wedge, while low-intensity regions (loss > 100 dB) are given as blank areas in the bottom. We clearly see how energy is being trapped in the wedge, and we also see how the four modes leak into the bottom as well-defined beams. The arrows start at the cut-off depth indicating the approximate beam directions.

Returning to the papers by Coppens and Sanders [15,16], they were particularly interested in determining the beam angle, a quantity that can be readily determined from this contour plot. The beam path for the last mode is here indicated by a dashed line that reveals a curved beam path close to the water/bottom interface (the near field), and a straight-line path only in the far field. Defining the beam angle as the angle between horizontal and a line connecting the point of cut-off at the water/bottom interface with the centre of the beam at any given distance from the interface, we see that the angle is dependent on the distance from the interface. Thus, the smallest beam angle in the near field is approximately 35% lower than the far-field angle. This fact seems to explain the discrepancy found between theory and experiment by Coppens and Sanders. They actually measured a 25 to 30% lower beam angle than predicted, but while their simplified theory predicts the far-field angle, the measurements were carried out in the near field, and thus according to Fig. 12 one should expect a difference of up to 35% between measured and predicted angles. This in turn is a result that definitely strengthens our confidence in the PAREQ model for handling sound propagation in a complicated, range-dependent ocean environment.

3.2 Seismic propagation

We now turn to an application that includes a seismic path. The Centre has been investigating the feasibility of sensing a sound source in the ocean by geophones placed on the ocean bottom in a coastal-water region [17]. If the bottom can support shear waves there will exist a surface wave that travels along the water/bottom interface. Indeed, a surface wave will exist at the interface between any two media if at least one of them can support shear waves. An important feature of these surface waves is that they have no frequency "cut-off", whereas, for a particular water depth, waterborne propagation cuts off below a frequency that is a function of the environmental conditions.

We have been investigating this phenomenon theoretically using the FFP program. Figure 13 displays a typical shallow-water environment: there is a 5 m sediment layer of fairly compact sand overlying a sedimentary rock basement. Hence, from the discussion above, two surface waves should exist: one at the water/sand interface and the other at the sand/rock interface. A characteristic feature of ideal surface waves is that they die off exponentially with distance from the interface. However, since

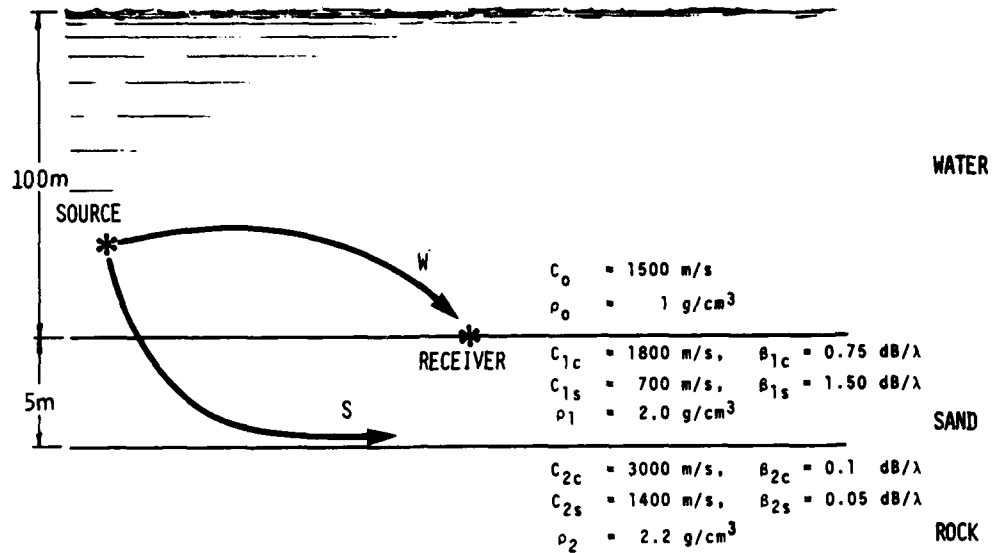


FIG. 13 ENVIRONMENTAL INPUT TO FFP FOR MODELLING SEISMIC VERSUS WATERBORNE PROPAGATION PATHS

each interface is in the presence of two other interfaces (we must include the water/air interface), the actual vertical distribution will be more complicated. Nevertheless, the FFP program is structured to handle this complicated coupled-interface wave-propagation problem as long as the interfaces are horizontal. We have calculated the propagation loss for a receiver placed on the bottom for both the waterborne path and the combined interface paths. Because of the high shear attenuation ($\beta_s = 1.5$ dB/wavelength) it turns out that the contribution from the Scholte wave* at the water/bottom interface is negligible. Hence the seismic path that dominates at the water/sand interface is the "non-ideal" Stoneley wave from the sand/

* To clarify nomenclature for this report, we give the names of the three types of "ideal" surface (or interface) waves that concern us. The most general of these is the Stoneley wave, which exists between two solids (materials that support shear). We use the connotation "ideal" to indicate that the two media are semi-infinite layers. If we set the shear speed of a solid to zero we have a liquid that just supports compressional waves. The interface wave between a liquid and a solid is often called a Scholte wave. Finally the interface wave between a solid and a vacuum is a Rayleigh wave; relative to a solid, air is considered as a vacuum.

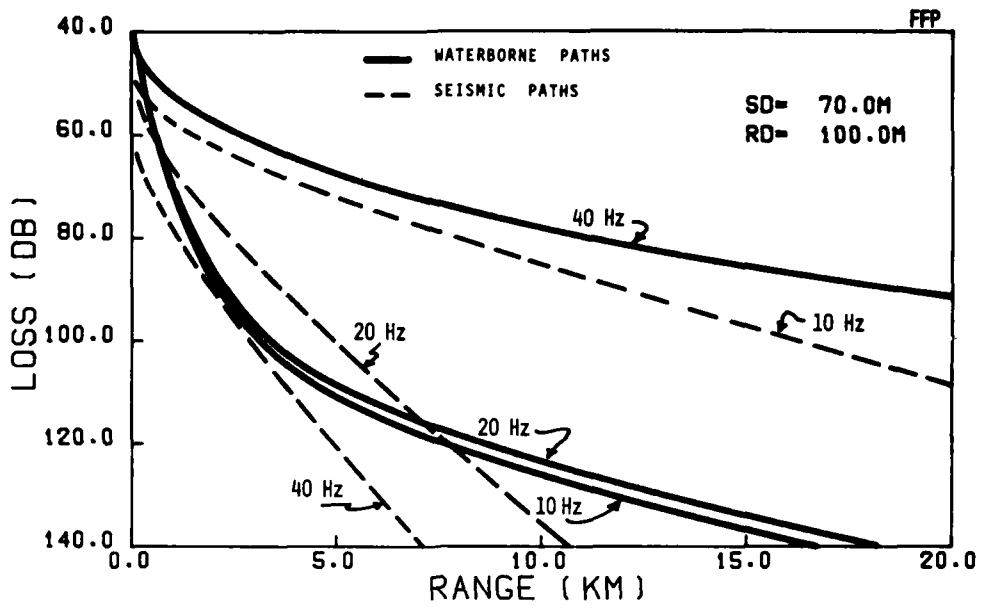


FIG. 14 PREDICTED LOSS VERSUS RANGE FOR SEISMIC AND WATERBORNE PATHS

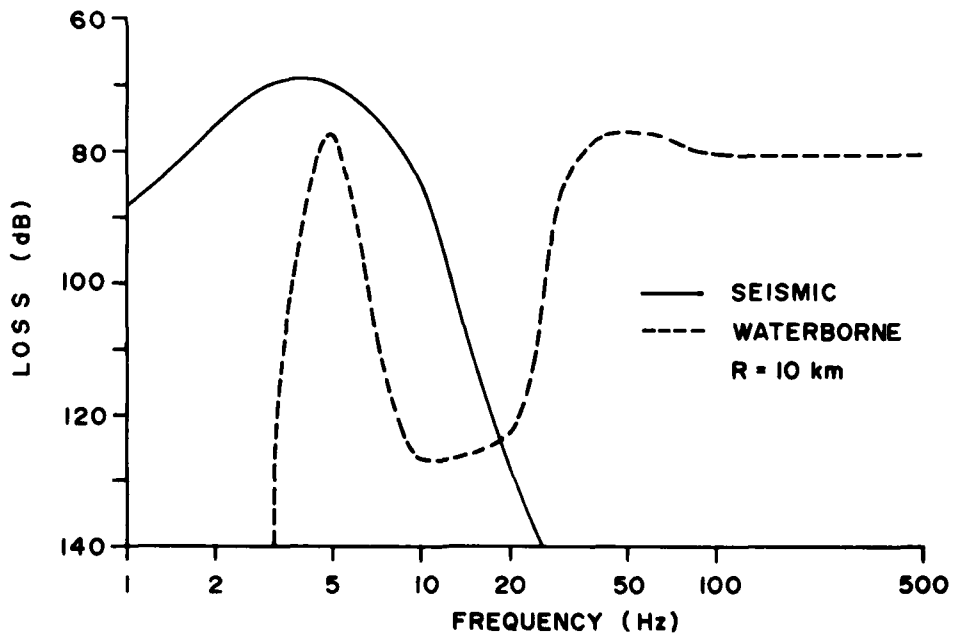


FIG. 15 PREDICTED LOSS VERSUS FREQUENCY FOR SEISMIC AND WATERBORNE PATHS

rock interface. Figure 14 shows waterborne and seismic mean propagation loss for 10, 20, and 40 Hz. At the low-frequency end the seismic paths propagate better than the waterborne paths while at the high-frequency end the opposite is predicted.

In Fig. 15 we have selected a range of 10 km and plotted the loss as a function of frequency. First we consider the waterborne path. At the high-frequency end there is little interaction with the sand and we have relatively good propagation (we are not considering such high frequencies where volume attenuation in the water column begins to dominate). As we decrease the frequency, penetration into the lossy sand sediment increases the propagation loss. However, below 10 Hz, which corresponds to a wavelength of 150 m in the water column, the acoustic field "sees" less and less of the lossy sand sediment and propagation gets better. Finally the waterborne field is cut-off below 5 Hz, the cut-off being mainly determined by the acoustic properties of the rock and the 105 m depth to the rock.

Next we consider the seismic path. For very low frequency (long wavelength) the interface wave does not see the water column or the sand. It is essentially a solid/vacuum interface wave — a Rayleigh wave. The loss increases with lower frequency (below 3 Hz) because the exponential tail in the rock grows with increasing wavelength and the loss is approximately proportional to the area of that tail in a lossy medium. This fall-off is not a cut-off but simply an attenuation phenomenon. As frequency increases, the tail gets smaller and we see a maximum (minimum loss) in the curve at about 4 Hz. At this point, the interface wave begins to sense the more lossy sand sediment and the water column, so that the loss begins to grow. Hence we are going from essentially a pure Rayleigh wave through a hybrid Rayleigh-Stoneley-Scholte wave region, which is a complicated wave that is not really any of the above three types of waves. Finally, as we asymptotically go to higher frequency, this wave becomes a Stoneley wave at the sand/rock interface: this is highly attenuated and its exponential tail into the sand sediment dies off rapidly with distance from the sand/rock interface so that it is undetectable at the sand/water interface.

Of course what has been presented in this chapter has been a model study of a hypothetical shallow-water environment. Seismic noise measurement indicates that noise levels begin to increase below 10 Hz. Concerning Fig. 15, it is believed, but yet to be demonstrated, that geophones will have about a 10 dB greater sensitivity for detecting these seismic waves over an ordinary hydrophone. If that turns out to be so, the seismic curve of Fig. 15 should in effect be displaced upward by 10 dB. Hence, seismic detection of a source radiating between 5 and 15 Hz would be greatly enhanced over conventional sonar techniques. Nevertheless it is interesting to note that a source radiating at about 20 Hz would be difficult to sense by any means.

4 NOISE MODELLING AT SAACLANTCEN

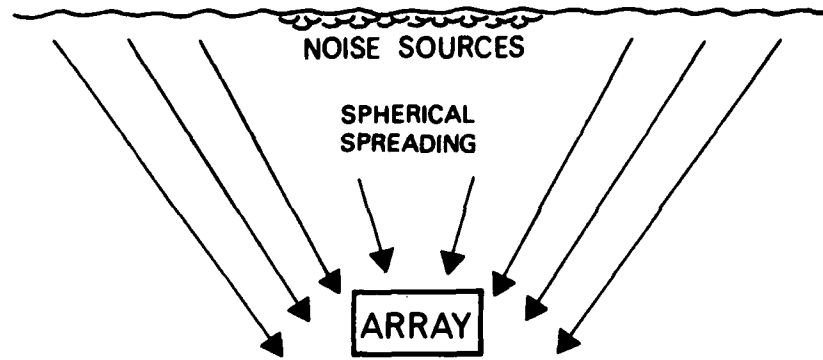
The Centre is involved in an experimental and theoretical programme to study the performance of various configurations of arrays in shallow water. Array gain is dependent on the spatial properties of both the signal and the noise field. In addition, any use of optimal array-processing techniques requires knowledge of the spatial correlation of the noise field. Therefore, in order to understand the performance of arrays in shallow water we must also understand the spatial properties of the noise field. A model for noise generated at the ocean surface has been constructed at the Centre (documentation in preparation) based on a theory [18] cooperatively developed at SAACLANTCEN and the US Naval Research Laboratory. The model is concerned with predicting the spatial properties of surface-generated noise in an environment where both bottom interaction and sound-speed profile are important.

Figure 16 depicts two models environments. In the past, near-surface (but far with respect to wavelength), deep-water noise models, see for instance [19], considered only direct paths. However, for a shallow-water environment we must include three types of paths: the direct arrivals, which do not interact with the bottom; paths that partially interact with the bottom; and the long-range contributions that can be described by a set of normal modes. In Fig. 16, θ_c refers to the critical angle of the bottom reflectivity curve. The first two paths mentioned above correspond to paths whose angles are greater than the critical angle. This corresponds to the so-called near-field (or "continuous spectrum") solution of the wave equation. As mentioned in Sect. 1.2, the FFP model includes the near-field as well as the far-field solution of the wave equation. However, we are very interested in the vertical structure of the noise field and it is impractical to extract the field as a function of depth from the full FFP solution. Hence, for the noise model we have combined algorithms from FFP and SNAP, relying mainly on the modularized architecture and input/output structure of SNAP. Subsequently the signal and noise field can be obtained in a non-redundant calculation. We now present the kind of results the model can output.

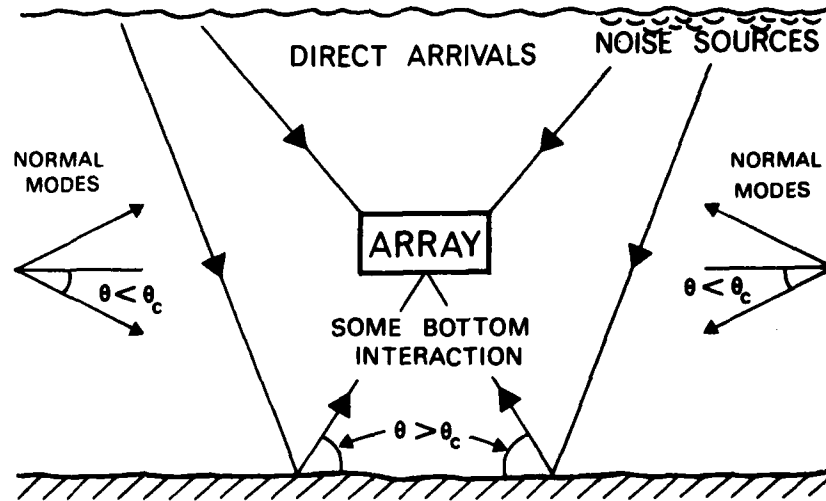
Figure 17 describes an upward-refracting, range-independent, shallow-water environment. Figure 18 displays the intensity output of the model. The intensity profiles for the noise and two possible signals are shown. The unknown parameter in the noise theory is the spectral strength of the surface-noise sources and so the noise field has been placed on the signal displays arbitrarily. (A program to determine the spectral strength experimentally is underway. In addition, a study of existing deep-water noise results is being made to estimate these strengths).

Referring back to Fig. 18, we are comparing noise at 200 Hz with two signals from point sources 30 km away and at depths of 20 m and 80 m. The model results indicate that for this environment (disregarding the spectral

FIGURE PAGE BLANK-NOT FILMED



SPATIAL DEEP WATER MODELS



SHALLOW WATER NOISE ENVIRONMENT

FIG. 16 DEEP AND SHALLOW-WATER MODEL ENVIRONMENTS FOR CALCULATING SURFACE-GENERATED NOISE LEVELS

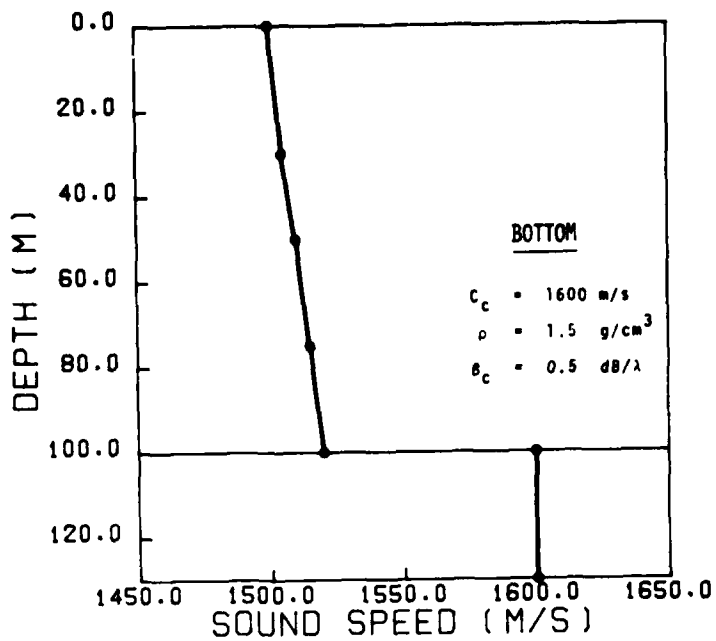


FIG. 17 ENVIRONMENTAL INPUT TO SHALLOW-WATER NOISE MODEL

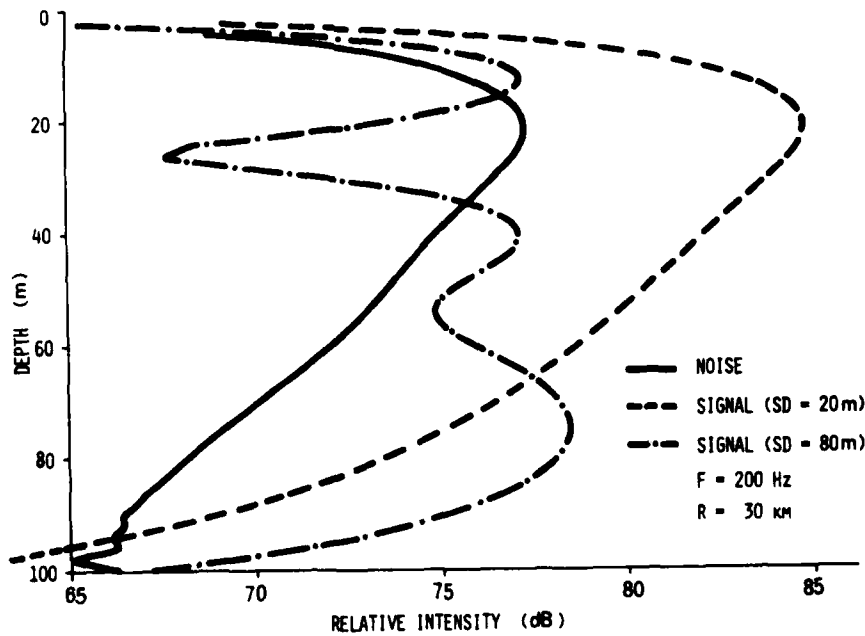


FIG. 18 PREDICTED NOISE AND FIELD INTENSITIES VERSUS DEPTH

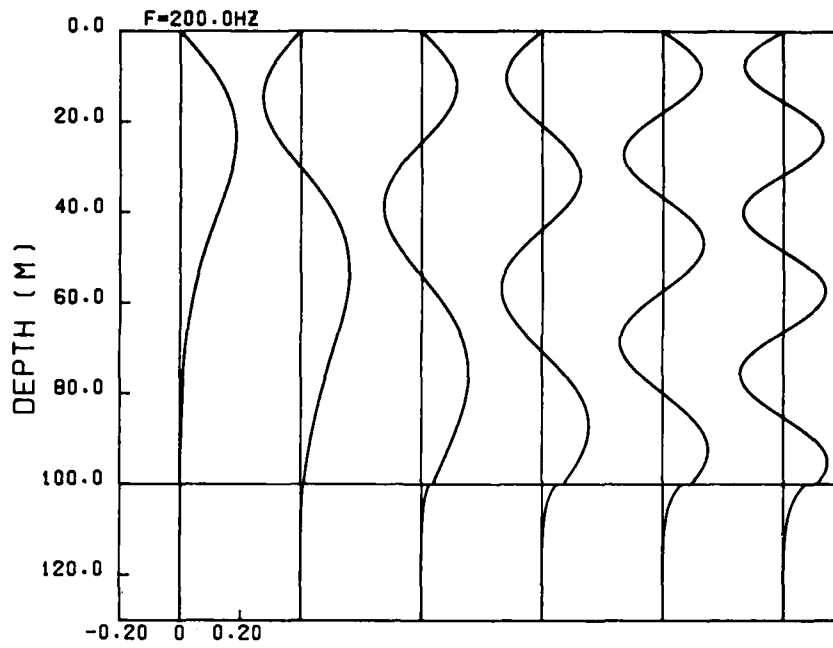


FIG. 19 MODAL DEPTH FUNCTION FOR FIRST 6 MODES

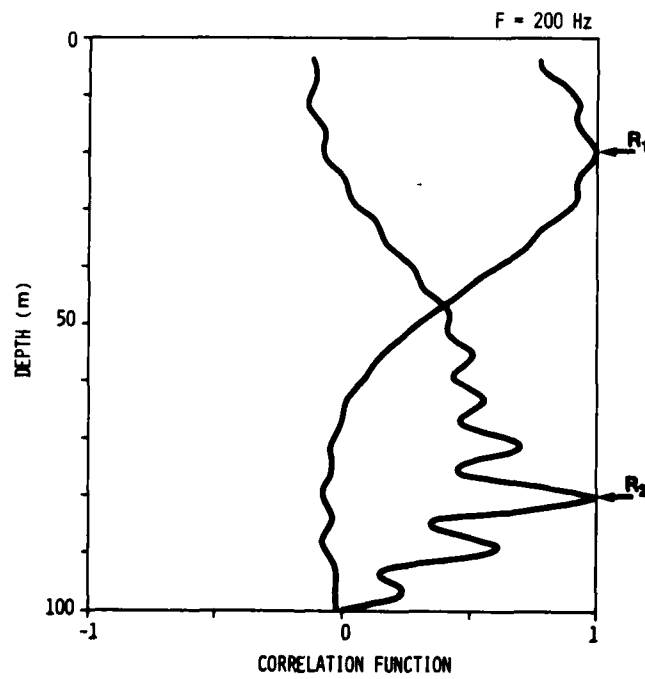


FIG. 20 SPATIAL CORRELATION FUNCTION OF NOISE FOR TWO DIFFERENT RECEIVER DEPTHS

strength of the noise sources) the optimum signal-to-noise ratio for detecting the shallow source is obtained by a shallow receiver. On the other hand, in order to detect a deep source we would do best by using a deep receiver. Hence, for this environment, placing the receiver at the depth of the source yields maximum signal-to-noise ratio.

We can understand the above results by looking at the normal modes present in such an environment. Figure 19 displays the first six normal modes. Because of the upward-refracting profile, the first mode is trapped in the water column (its amplitude function is between a depth of 0 and 100 m) and hence undergoes negligible attenuation due to bottom loss. All the other modes interact with the bottom to a much greater extent and therefore a signal from any significant distance will have all modes but the first attenuated out. Because the first mode propagates so well, the structure of the noise field will be dominated by the first mode, since it permits a large surface area of noise sources from long ranges to contribute. Hence the noise field in Fig. 18 has the same shape as the first mode in Fig. 19.

Similarly, a source placed at a depth of 20 m, which is at the maximum of the first mode, will at long distances only propagate the first mode. Therefore the noise and the signal field for a source at 20 m have the same shape. On the other hand, a source placed at 80 m where the first mode has very little amplitude, would tend to propagate the second and third modes, which explains the structure of the signal field in Fig. 19. This figure is not typical of all shallow-water environments but demonstrates how the model can be used to study and understand the relative properties of signal and noise intensities in a stratified ocean.

If we want to calculate the performance of an array of receivers we must also know the spatial correlation function (more formally known as the cross-spectral density function) of the noise field. Figure 20 displays such an output from the noise model for the same environment described by Fig. 17. The important feature of noise in a stratified medium is that the correlation of noise between two receiving points at a fixed separation distance varies with the absolute depth of the receiving pair. The correlation function is not spatially "homogeneous". In a simpler noise model of an isovelocity, infinitely deep ocean, the correlation function is independent of absolute depth and depends only on separation distance. Figure 20 displays the spatial inhomogeneity of a stratified medium. Here the noise at receiver R_1 is correlated with the noise at all other field points of the water column and the same is true for receiver R_2 . We see that the two correlation functions appear different, indicating this spatial inhomogeneity.

The amplitude of the envelope of the correlation function indicates approximately what is the longest array in which one can utilize optimal array-processing schemes. A simplistic picture of these techniques is to think of steering the array in a direction where there is very little noise. For example, if the envelope of the correlation function had an amplitude of one over the whole water column, that would indicate that the noise was a plane wave (from a single direction) and as long as one steered away from

that direction one would minimize reception of noise. If we arbitrarily pick a value of 0.5, or greater, that we need for the correlation function in order to utilize optimal processing techniques with a vertical array, we see from Fig. 20 that for noise rejection one could use a longer array in the upper half of the water column than in the lower half. Finally, we mention that the model also calculates horizontal correlation or arbitrary point-to-point correlation.

CONCLUSION

In this report we have presented a sequence of environmental modelling results with emphasis on coastal waters. We have tried to demonstrate the consistency among the models and how we understand their individual applicability to specific problems. While studies comparing models bring out their special idiosyncrasies, they also demonstrate quite clearly that the models are solving the same equation—the wave equation—in their various approximations. Furthermore, we now have a relatively good understanding of the range of validity of these approximations.

The model/data comparisons indicate that the models can indeed describe shallow-water propagation. These studies have also demonstrated the collective role of models and data to describe coastal-water regions acoustically. Having gained sufficient confidence in the models themselves, we have proceeded to do some simulation studies of various acoustical phenomena. Examples of such studies were presented in Chapters 3 and 4, demonstrating that such diverse phenomena as propagation over a sloping bottom, seismic propagation, and the distribution of surface-generated noise can be understood using the same physical principles. Hence the models can be used in multi-frequency parametric studies of different ocean environments.

Though it has often been said that very little is known about shallow-water acoustics, we do not believe this statement to be any longer valid. For example, we feel that we are not too far away from making actual "predictions". Research at SACLANTCEN will continue in model/data comparison; we then intend to make a prediction of winter propagation conditions using data available from a summer experiment and, to demonstrate the accuracy of the prediction, the winter experiment will be performed only after the prediction has been documented. Emphasis in future modelling efforts will be more concerned with noise and fluctuations, since we feel that propagation modelling is at a much more advanced stage than the former two phenomena.

REFERENCES

1. JENSEN, F.B. and FERLA, M.C. SNAP: the SACLANTCEN normal-mode acoustic propagation model, SACLANTCEN SM-121. La Spezia, Italy, SACLANT ASW Research Centre, 1979. [AD AO 67256]
2. MILLER, J.F. and INGENITO, F. Normal mode FORTRAN programs for calculating sound propagation in the ocean, NRL Memorandum Rpt. 3071. Washington, D.C., US Naval Research Laboratory, 1975.
3. INGENITO, F., FERRIS, R., KUPERMAN, W.A. and WOLF, S.N. Shallow-water acoustics, summary report (first phase), NRL Rpt 8179. Washington, D.C., US Naval Research Laboratory, 1978.
4. DINAPOLI, F.R. Fast field program for multilayered media, NUSC Report 4103. New London, Conn., Naval Underwater Systems Center, 1971.
5. KUTSCHALE, H.W. Rapid computation by wave theory of propagation loss in the Arctic Ocean, Rpt. CU-8-73. Palisades, N.Y., Columbia University, 1973.
6. TAPPERT, F.D. The parabolic approximation method. In: KELLER, J.B. and PAPADAKIS, J.S. eds. Wave Propagation and Underwater Acoustics. Lecture Notes in Physics 70. New York, Springer-Verlag, 1977: 224-287.
7. JENSEN, F.B. and KROL, H.R. The use of the parabolic equation method in sound propagation modelling, SACLANTCEN SM-72. La Spezia, Italy, SACLANT ASW Research Centre, 1975.
8. BROCK, H.K. The AESD parabolic equation model, NORDA TN-12. NSTL Station, Miss., Naval Ocean Research and Development Activity, 1978.
9. CORNYN, J.J. CRASS: a digital-computer ray-tracing and transmission-loss-prediction system, NRL Report 7621 (Vol. 1, overall description) and NRL Report 7642 (Vol. 2, user's manual). Washington, D.C., Naval Research Laboratory, 1973.
10. SPOFFORD, C.W. The FACT model, MC Report 109. Arlington, Va., Office of Naval Research, 1974.
11. WEINBERG, H. Navy interim surface ship model (NISSM) II, NUSC TR-4527. New London, Conn., Naval Underwater Systems Center, 1973.

12. BACHMANN, W. and RAIGNIAC, B. de. Calculations of reverberation and average intensity of broadband acoustic signals in the ocean by means of the RAIBAC computer model. Journal Acoustical Society America 59, 1976: 31-38.
13. HASTRUP, O.F. Reflection of plane waves from a solid multilayered damping bottom, SACLANTCEN TR-50. La Spezia, Italy, SACLANT ASW Research Centre, 1966. [AD 479 437]
14. HASTRUP, O.F. Impulse response of a layered bottom, SACLANTCEN TR-85. La Spezia, Italy, SACLANT ASW Research Centre, 1967. [AD 811 104]
15. COPPENS, A. The model: transmission of sound into a fast fluid bottom from an overlying fluid wedge. In: Proceedings of workshop on seismic propagation in shallow water. Arlington, Va., Office of Naval Research, 1978.
16. SANDERS, J. The experiment: transmission of acoustic waves into a fast fluid bottom from a converging fluid wedge. In: Proceedings of workshop on seismic propagation in shallow water. Arlington, Va., Office of Naval Research, 1978.
17. RAUCH, D. Seismic interface waves in coastal waters. SACLANTCEN document in preparation.
18. KUPERMAN, W.A. and INGENITO, F. Spatial correlation of surface generated noise in a stratified ocean. Paper submitted to JASA for publication.
19. CRON, B.F. and SHERMAN, C.H. Spatial-correlation functions for various noise models. Journal Acoustical Society America 34, 1962: 1732-1736.

[Note: Documents with AD numbers may be obtained from the US National Technical Information Service or national outlets in other nations.]